Supplemental Information

Cell surface photoengineering enables modeling of glycocalyx shedding dynamics

[1,#]Sean C. Purcell, [1,†,#]Michelle H. Zhang, [1,‡]Daniel J. Honigfort, [1]Hans Jefferson C. Ng, [1]Austen L. Michalak, and [1,2]Kamil Godula*

[1]Department of Chemistry and Biochemistry, [2]Glycobiology Research and Training Center, University of California San Diego, 9500 Gilman Drive, La Jolla, CA 92093.

[†]Current address: Western Michigan University, 300 Portage St., Kalamazoo MI, 49007

[‡] Current address: Element Biosciences, 9880 Campus Point Dr., San Diego CA, 92121

[#]These authors contributed equally.

Corresponding author: kgodula@ucsd.edu

Table of Contents

Abbreviations

CAM: cerium ammonium molybdate stain

CHO cells: chinese hamster ovary epithelial cells

Chol: cholesterol

CuAAC: copper(I)-catalyzed azide alkyne cycloaddition

DCM: dichloromethane

DIPEA: N,N-Diisopropylethylamine

DMF: dimethylformamide

DMSO: dimethylsulfoxide

DP: degree of polymerization

DPBS: Dulbecco's phosphate buffered saline

ECH: epichlorohydrin

FBS: fetal bovine serum

GP: glycopolymer

GPC: gel permeation chromatography

HRMS: high resolution mass spectroscopy

IR: infrared spectroscopy

M_n: number average molecular weight

M_w: weight average molecular weight

NHS: N-hydroxysuccinimide

NMR: nuclear magnetic resonance

NPCL: nonphotocleavable

PCC: Pearson's correlation coefficient

PCL: photocleavable

pECH: poly(epicholorhydrin)

PEG: polyethylene glycol

p(GA): poly(glycidyl azide)

RCA: *Ricinus communis agglutinin I*

$TBAN_3$: tetrabutylammonium nitride

THF: tetrahydrofuran

TLC: thin layer chromatography

wt: wild type

Ø: no cholesterol endgroup

Đ: polydispersity index

Materials. All chemicals, unless otherwise stated, were purchased from Sigma Aldrich and used as received. Cuprisorb resin was purchased from SeaChem Labs. Reaction progress was monitored by analytical thin-layer chromatography (TLC, Merck silica gel plates) with UV illumination or via staining with CAM, ninhydrin, or $KMnO_4$. CHO Lec8 and CHO Pro5 cells used were obtained from ATCC (CRL-1737 and CRL-1781, respectively). Biotin-labeled *Ricinus communis agglutinin I* was purchased from Vector Labs (B-1085-5) and streptavidin Alexafluor488 conjugate was purchased from ThermoFisher Scientific (S11223).

Instrumentation. Column chromatography was performed on a Biotage Isolera One automated flash chromatography system. Nuclear magnetic resonance (^1H and ^{13}C NMR) spectra were recorded on Bruker 300 MHz and Jeol 500 MHz NMR spectrometers. Spectra were recorded in

$CDCl_3$ or D_2O at 293K and are reported in parts per million (ppm) on the δ scale relative to residual solvent as an internal standard (for ^1H NMR: $CDCl_3$ = 7.26 ppm, D_2O = 4.79 ppm, for ^{13}C NMR: $CDCl_3$ = 77.0 ppm, CD_3OD = 49.0 ppm). HRMS (high-resolution mass spectrometry) analysis was performed on an Agilent 6230 ESI-TOFMS in positive ion mode. UV-Vis spectra were collected in a quartz cuvette using a Thermo Scientific Nanodrop2000c spectrophotometer. IR spectroscopy was performed on a Nicolet 6700 FT-IR spectrophotometer (Thermo Scientific). Size exclusion chromatography (SEC) was performed on a Hitachi Chromaster system equipped with an RI detector and two 5 μm, mixed bed, 7.8 mm I.D. x 30 cm TSK gel columns in series (Tosoh Bioscience) using an isocratic method with a flow rate of 0.7 mL/min in DMF (0.2% LiBr, 70 °C). Live cell flow cytometry analysis was performed using a FACSCalibur or FACSCanto II system (BD Biosciences). Data were collected using FACS Diva software and analyzed in FlowJo. Microscopy was performed on either a Keyence BZX800 epifluorescent microscope or a ThermoScientific EVOS imaging system. Images were analyzed using ImageJ. UV treatment was administered with a handheld 15W lamp (λ = 365nm) at < 2cm distance from the sample.

CHEMISTRY

Scheme S1. Synthesis of control GPs. Analogous synthetic schemes for non-photocleavable polymer control **GP-NPCL** (A) and for control polymer lacking a membrane anchor **GP-∅** (B). General **GP** elaboration[1] from **P1** (**ECH** polymerized as described by Gervais, et.al.[2]).

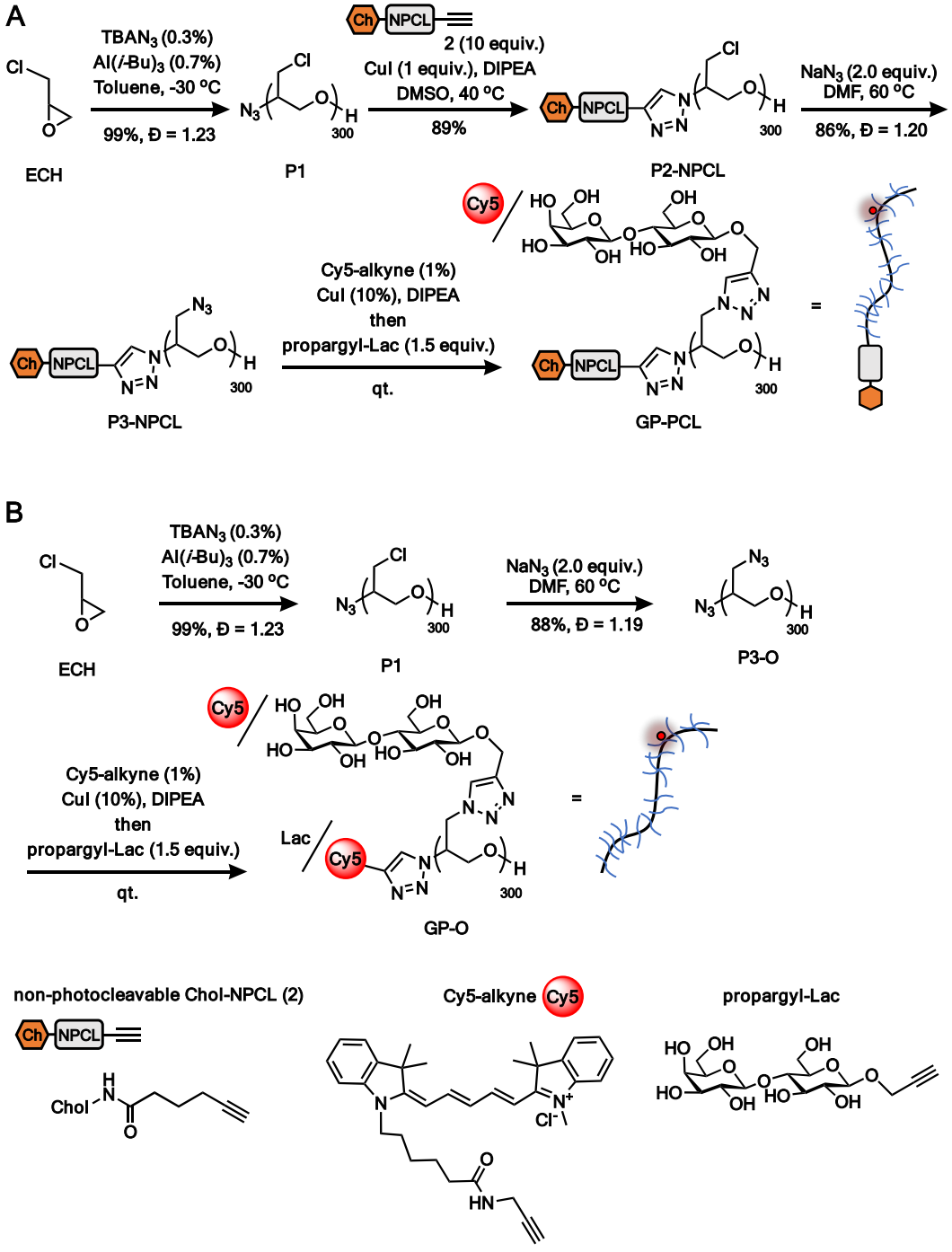

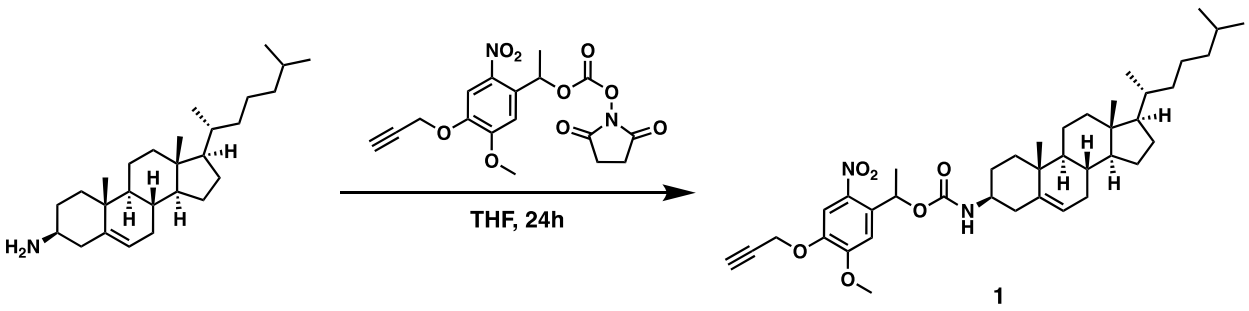

Synthesis of Chol-PCL (1). To a vacuum dried 1-dram glass vial with a magnetic stirrer was added 1-(5-Methoxy-2-nitro-4-prop-2-ynyloxyphenyl)ethyl N-succinimidyl carbonate[3] (0.0357 g, 0.091 mmol, 1 equiv) and Chol-amine[4] (3β-cholest-5-en-3-amine, 0.0352 g, 0.091 mmol, 1 equiv). Anhydrous tetrahydrofuran (0.50 mL) was added, and the reaction proceeded at ambient temperature for 18hr, during which time progress was monitored by TLC. The mixture was evaporated under reduced pressure and purified by normal phase flash chromatography in EtOAc/Hexanes (1:4). The purified product was concentrated to yield Chol-PCL **1** (0.0603 g, 60%). ^{1}H NMR ($CDCl_3$, 500 MHz) δ (ppm): 7.86-7.69 (s, 1H), 7.08-6.97 (s, 1H), 6.47-6.28 (d, 1H), 5.41-5.25 (br, 1H), 4.87-4.77 (d, 2H), 4.71-4.61 (m, 1H), 4.04-3.92 (s, 3H), 3.47-3.29 (br, 1H), 2.61-2.54 (m, 1H), 2.40-1.72 (br, 8H), 1.66-0.77 (br, 48H), 0.72-0.57 (s, 3H). ^{13}C NMR (500 MHz, $CDCl_3$) δ (ppm): 154.33, 153.99, 153.78, 153.66, 153.61, 153.54, 153.47, 152.35, 145.30, 140.02, 139.36, 135.36, 122.12, 110.13, 108.10, 68.70, 56.89, 56.63, 56.41, 56.07, 51.32, 49.96, 39.68, 39.51, 36.16, 35.81, 31.81, 28.25, 28.04, 23.83, 22.86, 22.59, 19.35, 18.71, 11.87. Calculated $C_{40}H_{58}N_2O_6$, 662.43, $[M+Na]^+$:685.42. HRMS found: 685.47. UV–Vis absorbance at 370 nm of **1** (CH_2Cl_2, 10 μg/mL) = 0.145.

Figure S1. ^{1}H NMR spectra (500mHz, $CDCl_3$) of **1**.

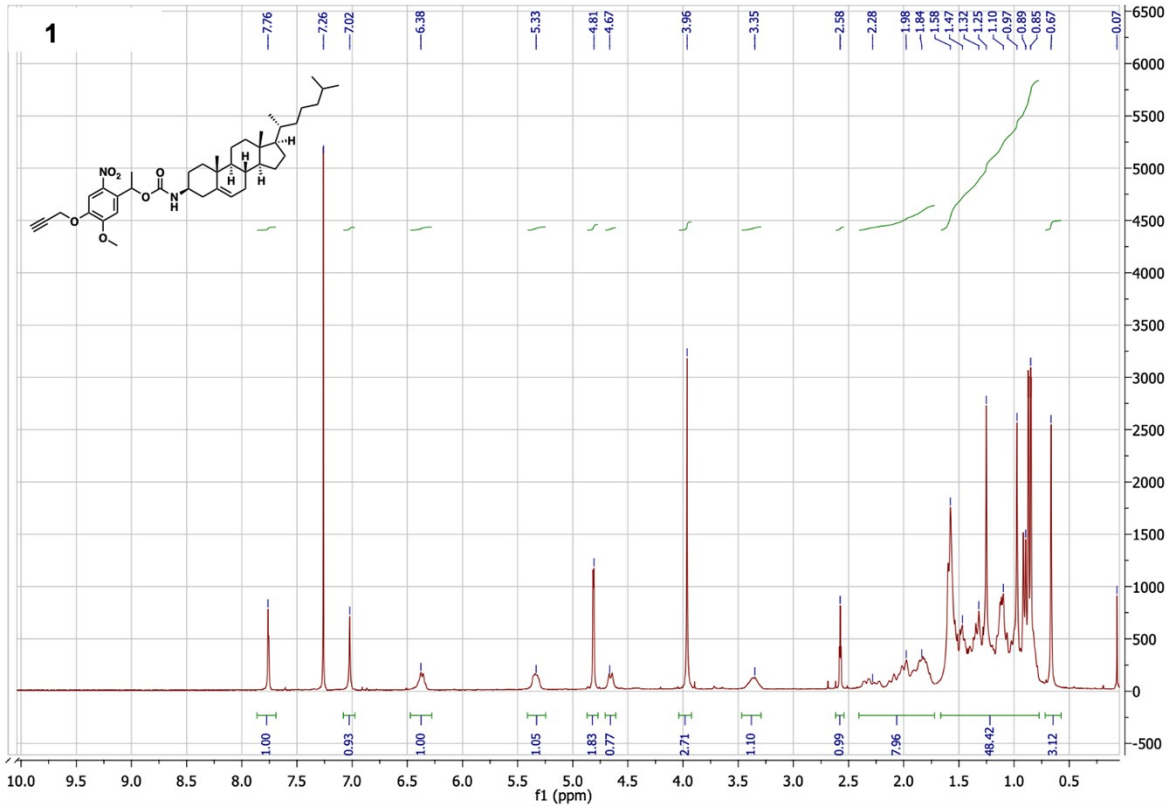

Figure S2. ^{13}C NMR spectra (500mHz, $CDCl_3$) of **1**.

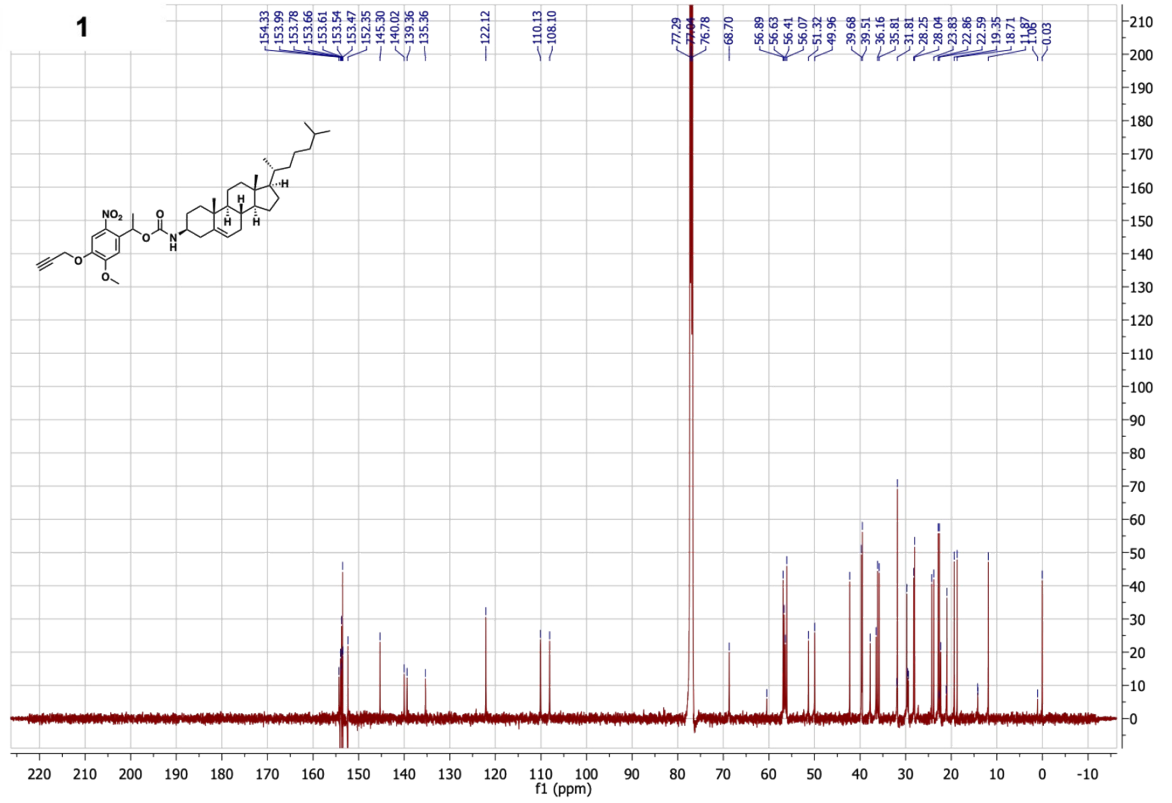

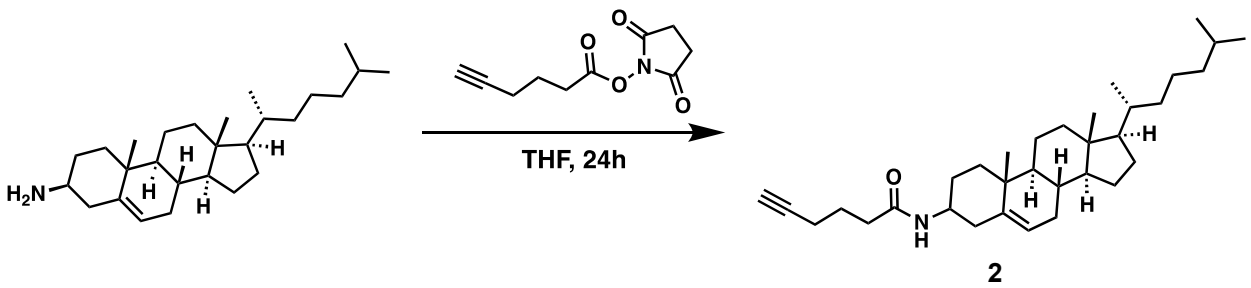

2

Synthesis of Chol-NPCL (2). A vacuum dried 1-dram glass vial with a magnetic stirrer was charged with hexynoic acid NHS-ester[5] (0.0263 g, 0.126 mmol, 1.00 equiv) and Chol-amine[4] (3β-cholest-5-en-3-amine, 0.0485 g, 0.126 mmol, 1.00 equiv). Anhydrous tetrahydrofuran (0.63 mL) was added and the reaction proceeded at ambient temperature for 18hr, during which time progress was monitored by TLC. The mixture was evaporated under reduced pressure and purified by normal phase flash chromatography in EtOAc/Hexanes (1:4). The purified product was concentrated to yield Chol-NPCL **2** (0.0449 g, 74%). ^{1}H NMR ($CDCl_3$, 500 MHz) δ (ppm): 5.49-5.19 (s, 1H), 3.87-3.45 (s, 1H), 2.94-2.64 (br, 4H), 2.49-2.16 (br, 4H), 2.05-1.77 (br, 6H), 1.63-1.41 (br, 4H), 1.39-0.61 (br, 34H). ^{13}C NMR (500 MHz, $CDCl_3$) δ (ppm): 11.87, 17.79, 18.72, 19.37, 22.59, 22.86, 24.19, 28.04, 31.83, 35.32, 37.81, 39.35, 39.51, 42.28, 49.61, 50.02, 56.07, 56.65, 69.18, 83.64, 122.04, 140.14, 153.61, 153.75, 153.77, 153.87, 154.06 171.29. Calculated $C_{33}H_{53}NO$, 479.41, $[M+H]^+$: 480.42. HRMS found: 480.5033.

Figure S3. ^{1}H NMR spectra (500mHz, $CDCl_3$) of **2**.

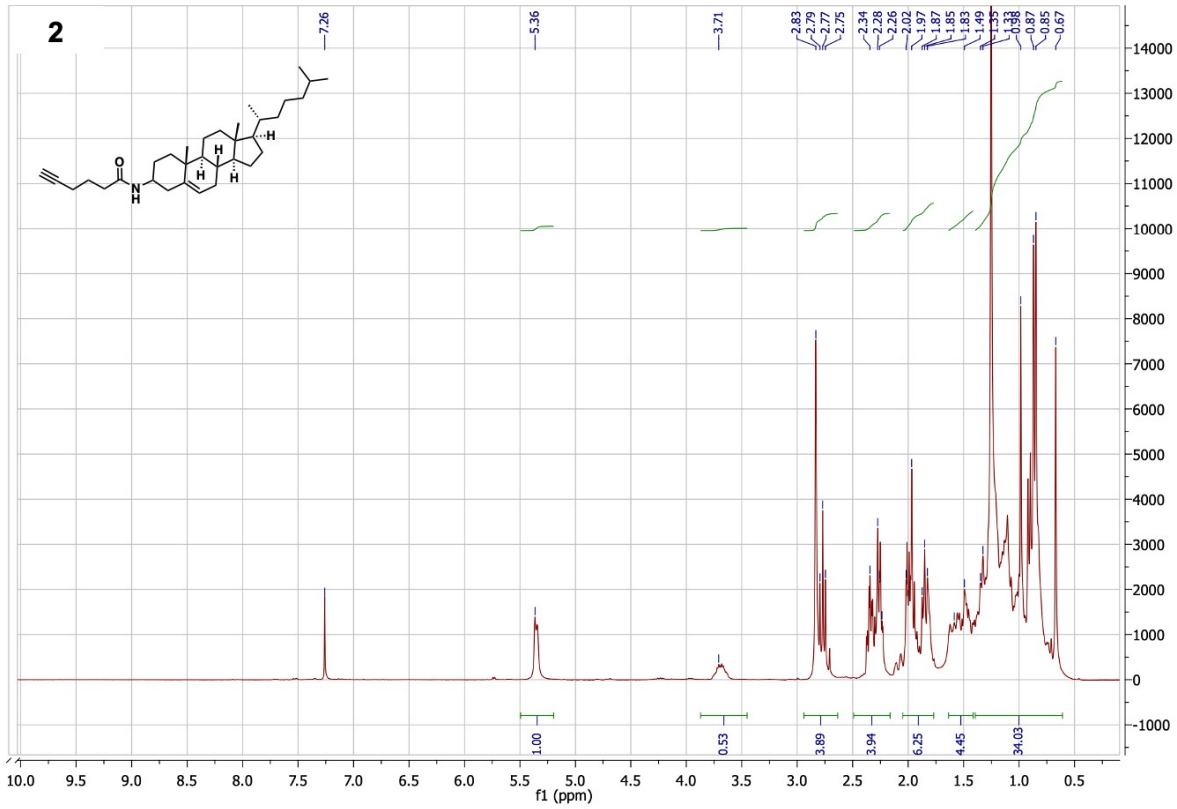

Figure S4. ^{13}C NMR spectra (500mHz, $CDCl_3$) of **2**.

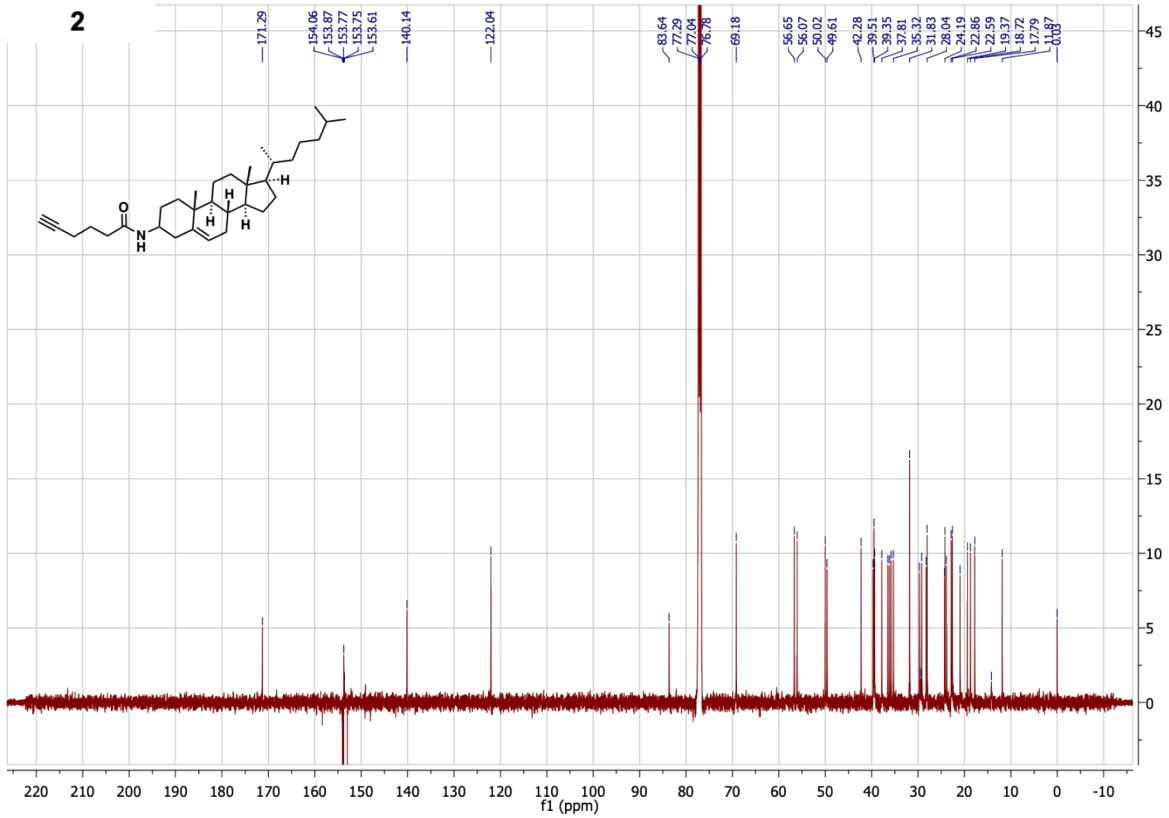

Characterization of GPs and their synthetic intermediates P1, P2, and P3

Figure S5. ^{1}H NMR spectra (500mHz, $CDCl_3$) of p(ECH) backbone **P1**.

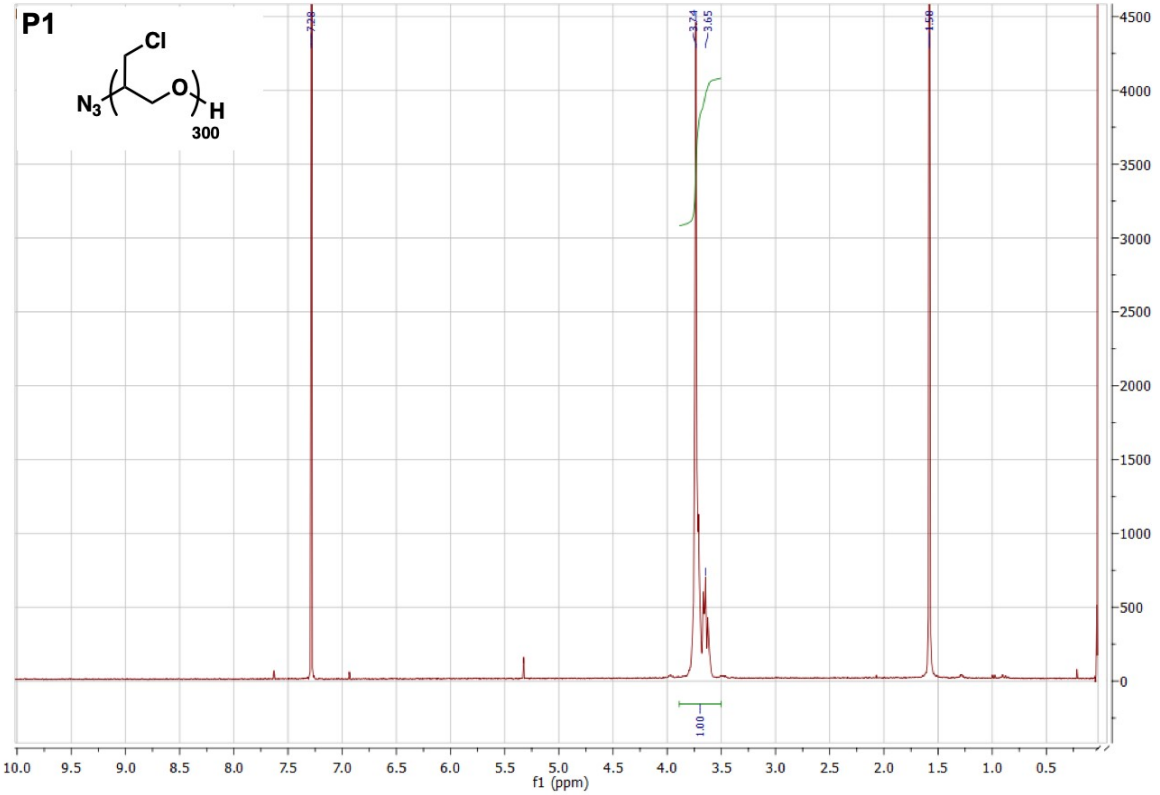

Figure S6. ^{1}H NMR spectra (500mHz, $CDCl_3$) of **P2** polymer intermediates.

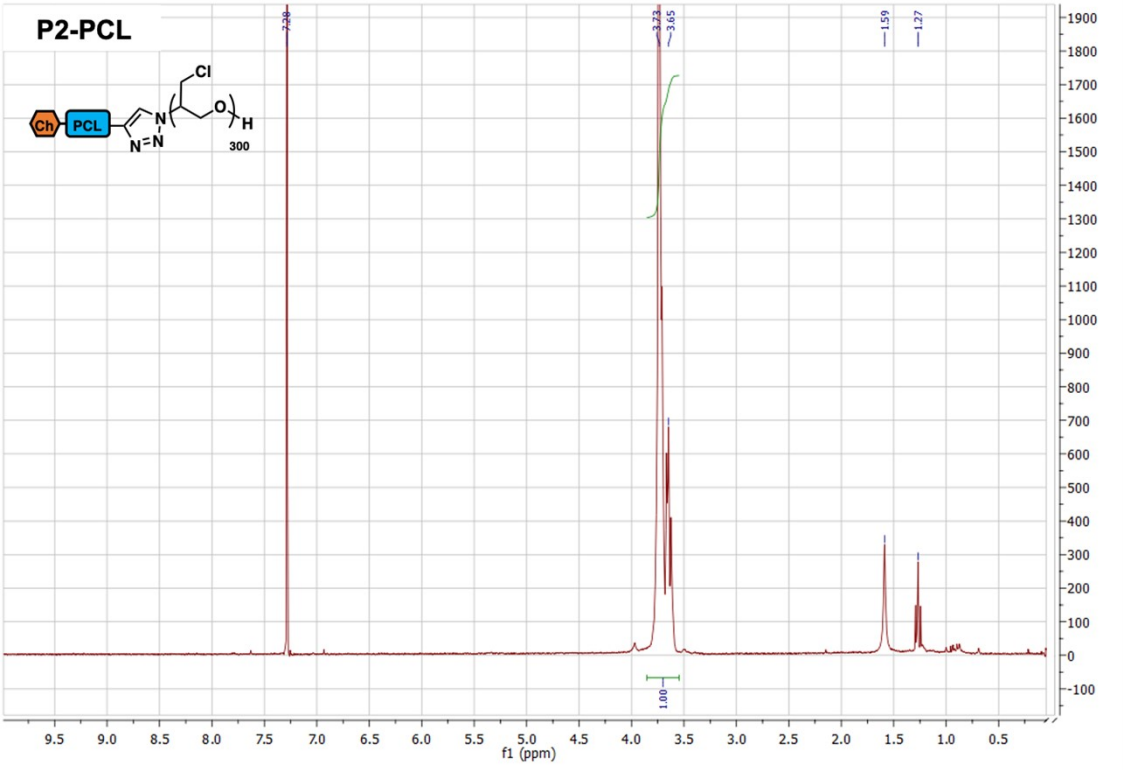

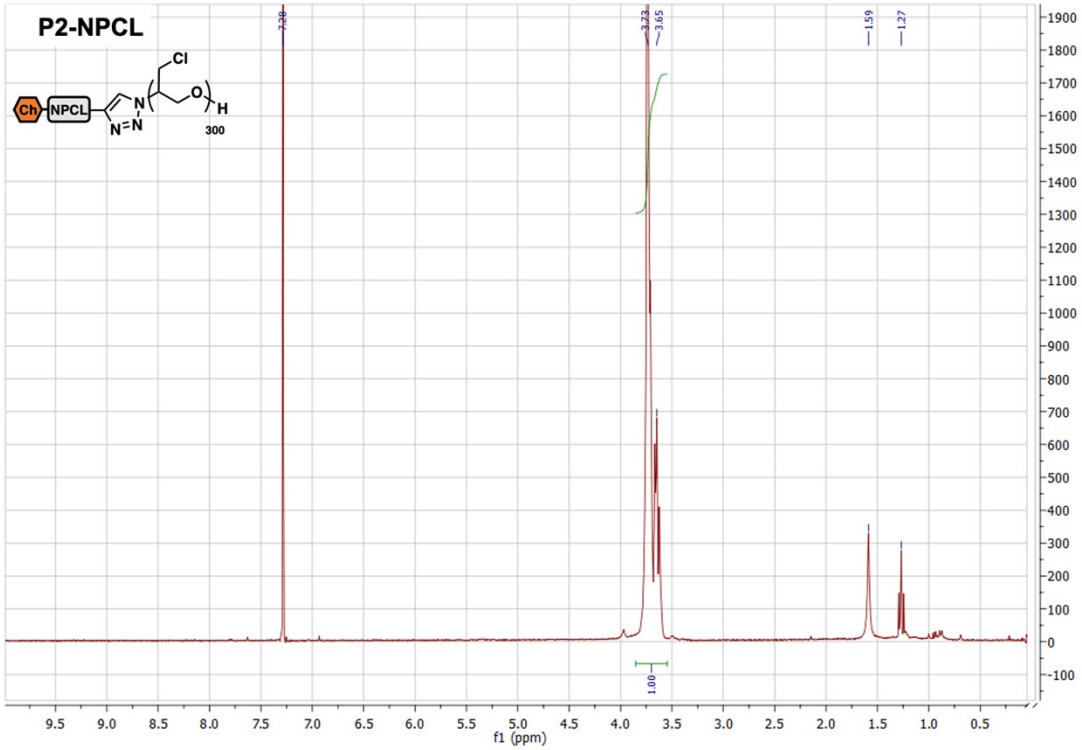

Figure S7. ^{1}H NMR spectra (500mHz, $CDCl_3$) of **P3** polymer intermediates.

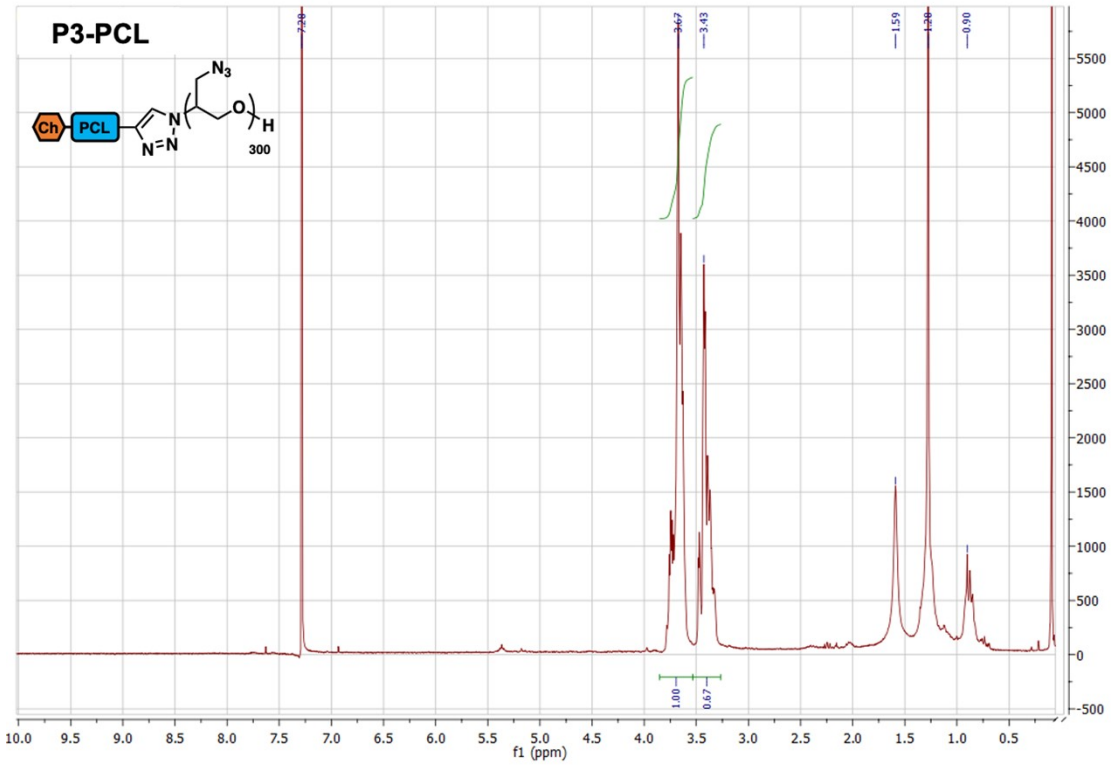

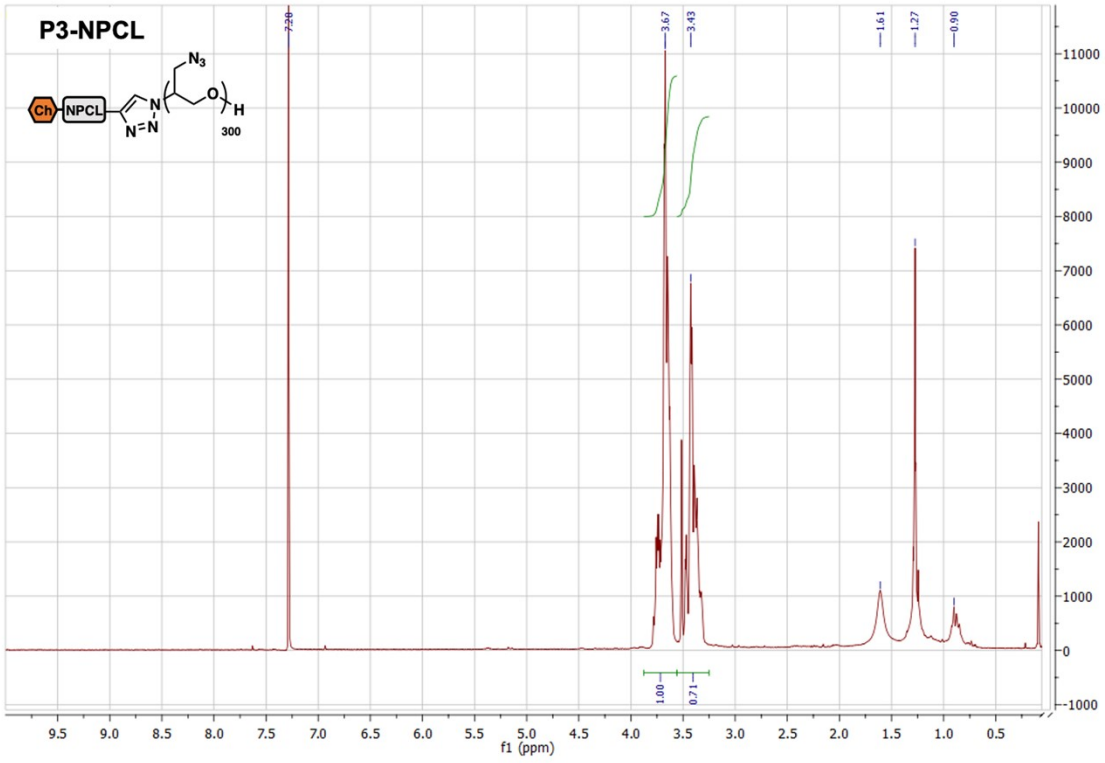
P3-NPCL
Ch
NPCL
N3
O
H
300
7.28
3.67
3.43
1.61
1.27
0.90
1.00
0.71
f1 (ppm)

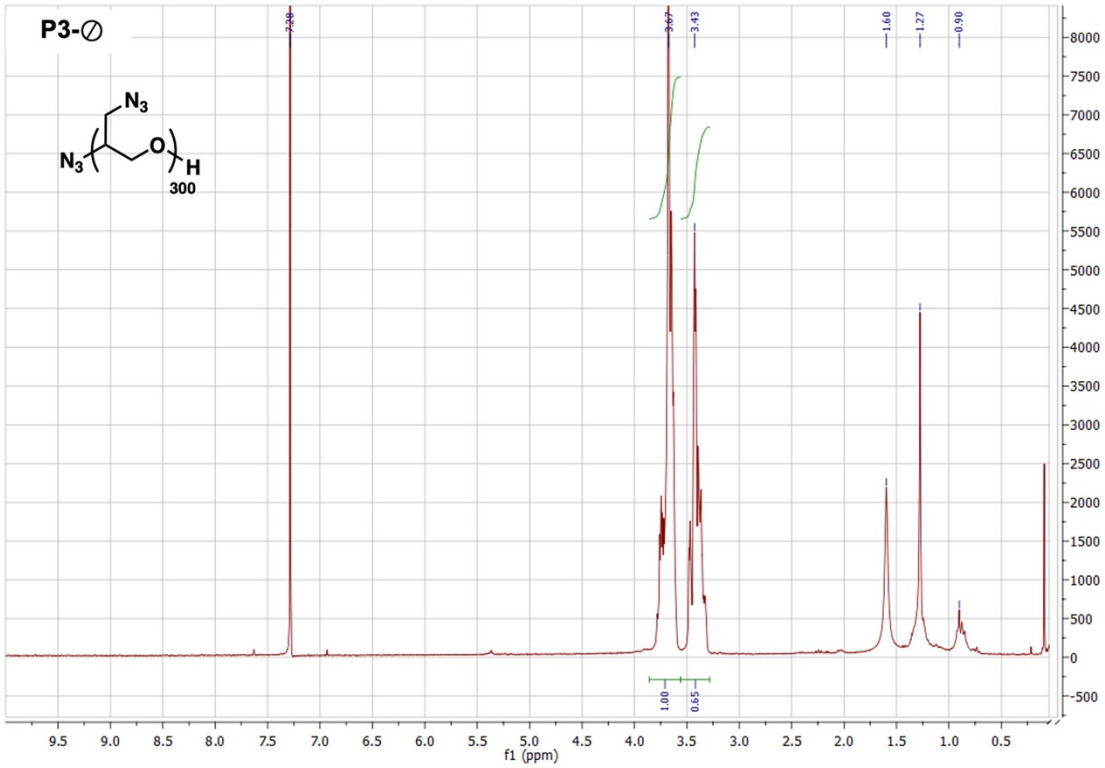
P3-∅
N3
N3
O
H
300
7.28
3.67
3.43
1.60
1.27
0.90
1.00
0.65
f1 (ppm)

Figure S8. ^{1}H NMR spectra (500mHz, D_2O) of **GPs**.

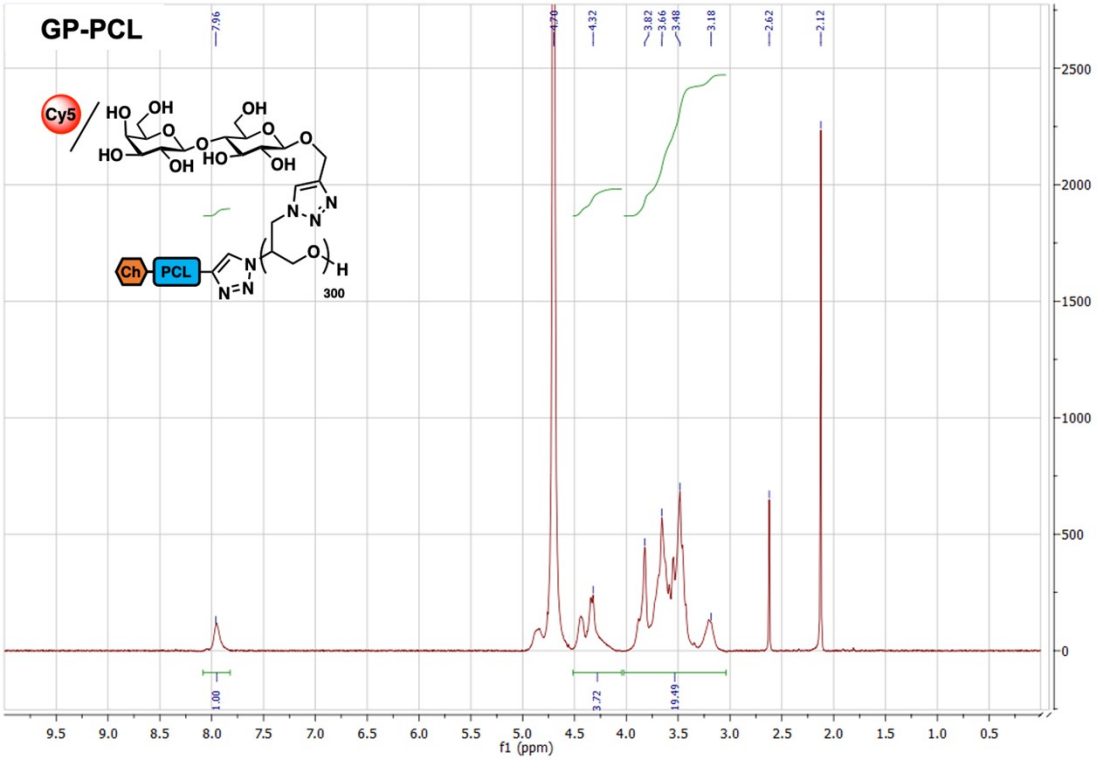

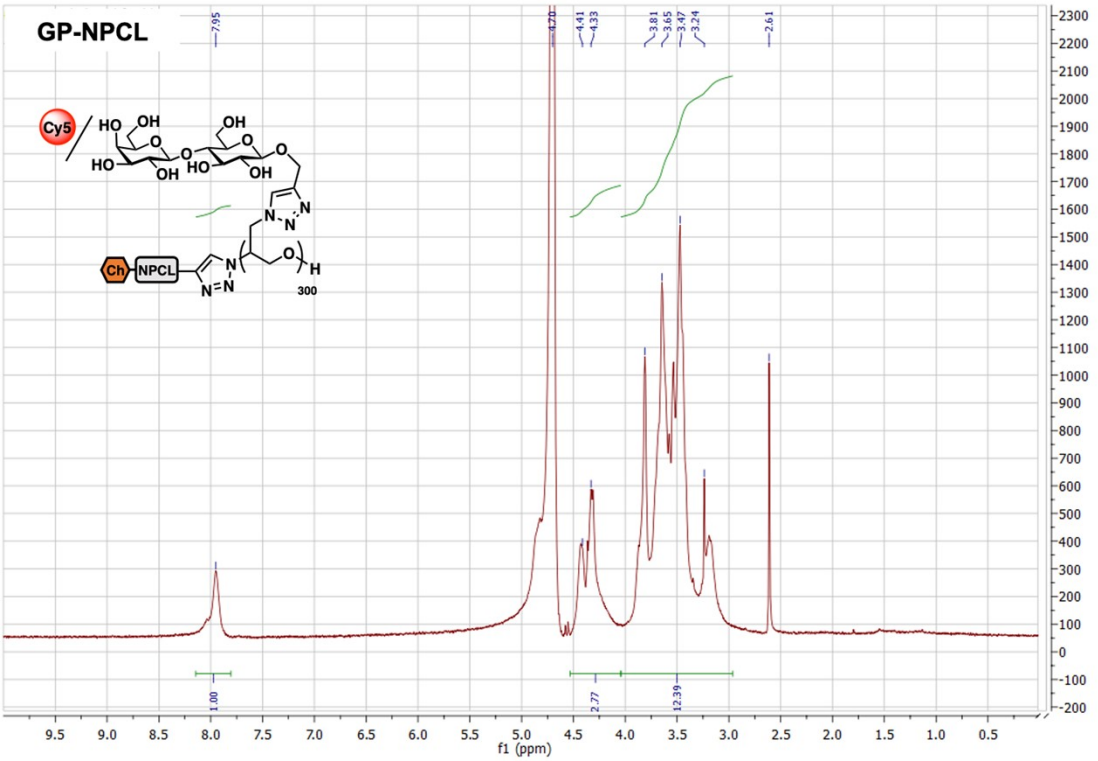

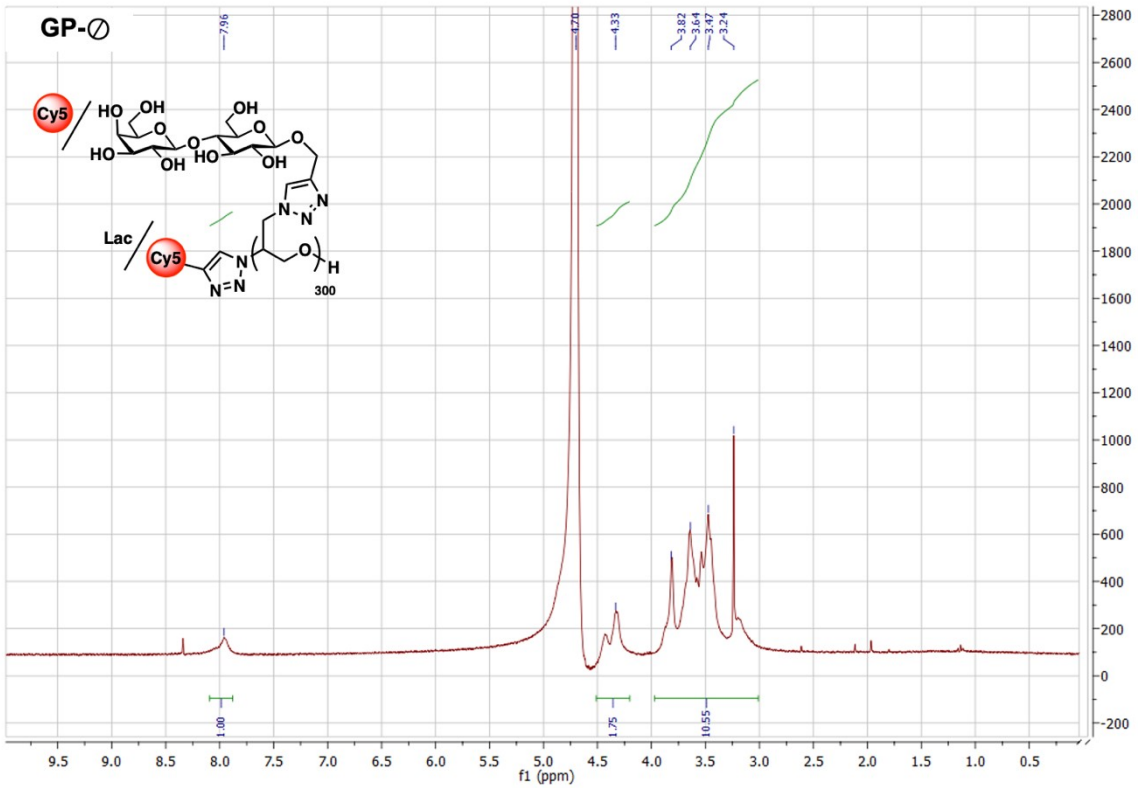
GP-∅
Cy5
HO
OH
O
HO
OH
O
HO
OH
O
O
N
N
N
Lac
Cy5
N
N
N
O
H
300
7.96
4.70
4.33
3.82
3.64
3.47
3.24
1.00
1.75
10.55
f1 (ppm)

Figure S9. IR spectra showing chain-end modification of polymer **P1**.

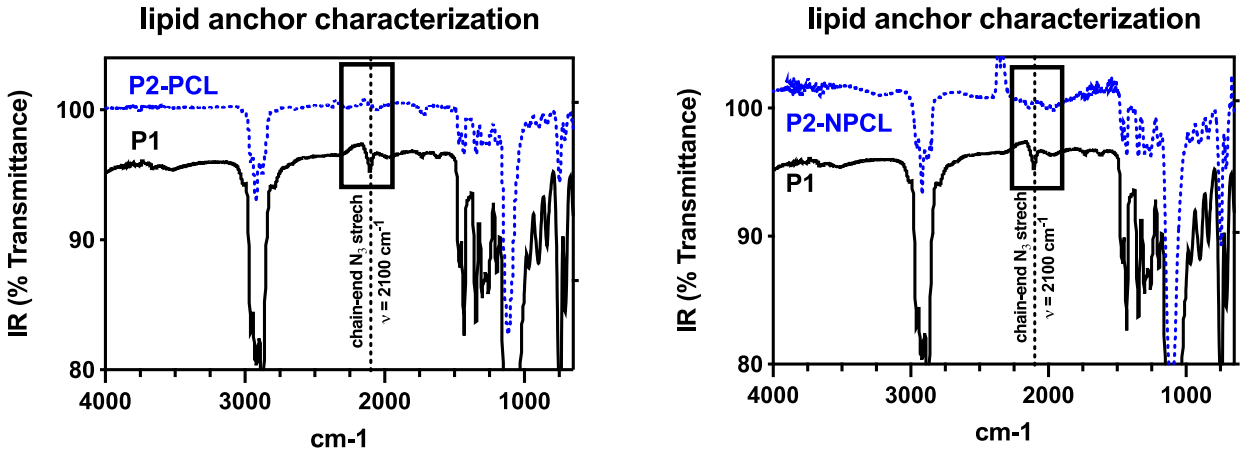

Figure S10. IR spectra showing side chain modification of **P3** polymer intermediates.

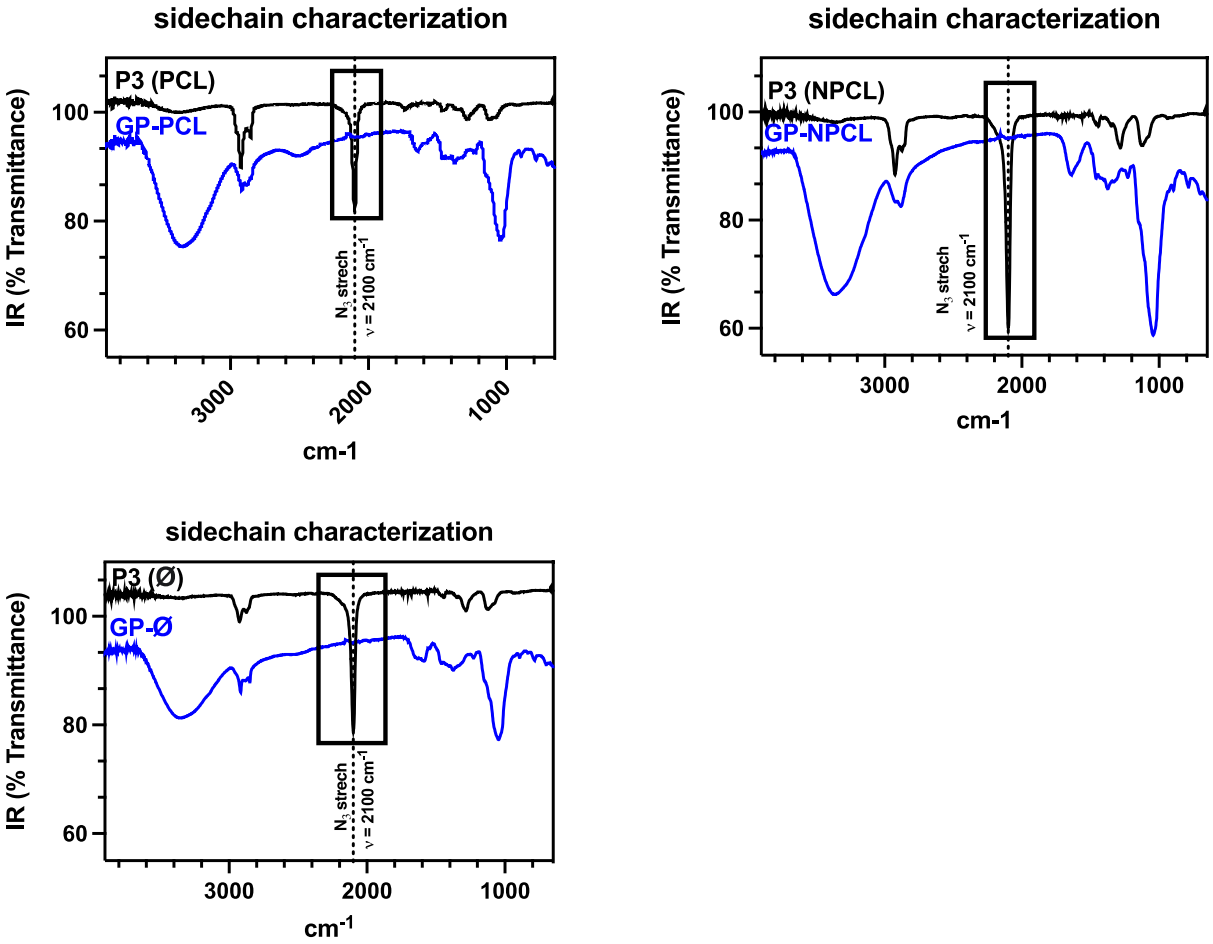

Figure S11. GPC spectrum (DMF, 0.2% LiBr) of **P1** and **P3** polymer intermediates.

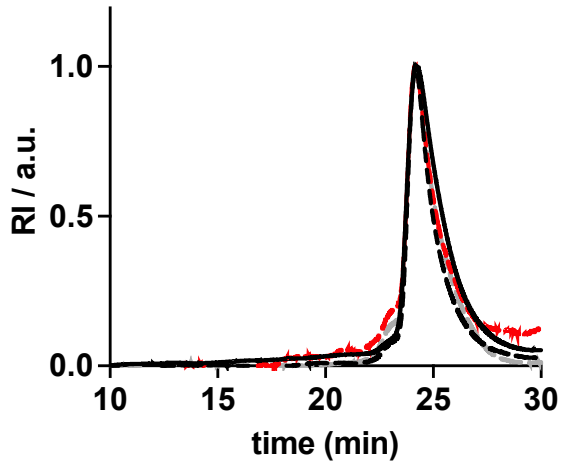

	M_n (kDa)	Đ
P1	27.7	1.23
P3-PCL	29.2	1.21
P3-NPCL	30.0	1.20
P3-O	30.6	1.19

Figure S12. P2-PCL photocleavage kinetic characterization. The photocleavage of the polymer intermediate **P2-PCL** (100 μg/mL) with light at λ = 365 nm was analyzed by UV spectroscopy (A). The change in absorbance at λ = 380 nm over time was used to determine the rate of photocleavage (B, $k = 5.1 \pm 2.3$ min^{-1}).

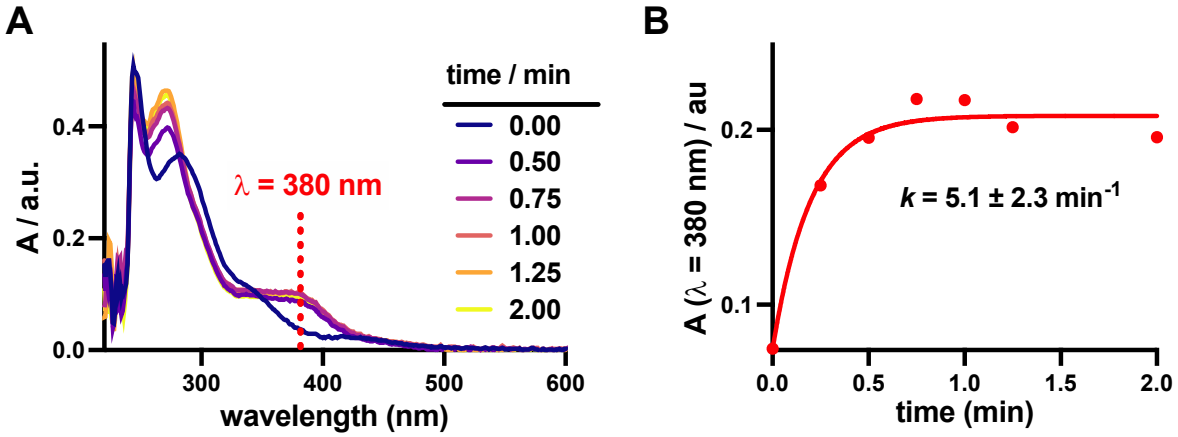

BIOLOGY

General methods. All biological reagents were purchased from Gibco (ThermoFisher) unless otherwise stated. Cells were cultured at 37 °C and 5% CO_2 following standard tissue culture practices. Chinese Hamster Ovary (CHO) cells (*wt* Pro5 and Lec8) were cultured in MEMα media supplemented with 10% FBS, 100 U/mL penicillin, and 100 U/mL streptomycin. Cells were passaged utilizing 0.25% trypsin-EDTA every 2-4 days to achieve desired confluency for or flow cytometry or microscopy on tissue-culture treated lab plastics.

Cells were washed with DPBS ($^{+}$Ca/$^{+}$Mg) and flow cytometry was performed on living cells with > 10,000 events per sample analyzed. All data were collected in biological triplicate. Live-dead cell analysis was performed using a commercial dead cell stain kit (Thermo-L34970) and a heat-treated control condition.

All microscopy experiments were performed in biological triplicate with 5 or more representative micrographs collected per replicate in all channels analyzed (BF, Hoechst, Cy5, and GFP). Photopatterned wells were masked using black electrical tape and ensuring that adhesive did not contact the imaging surface directly. ImageJ software was utilized to analyze all images. Cell nuclei were stained with Hoechst 33342. For photopatterning, the profile of Cy5 mean fluorescent intensity was recorded across the stitched images and bins were calculated at 100px width extending in both directions from the mask boundary. Prism software was utilized to fit a smoothed average across bins as a function of distance from the photomask. For lectin crosslinking experiments Cy5 and AF_{488} mean fluorescent intensity were quantified as a function of area and normalized to cell count. Plotted values represent the normalized Cy5 mean fluorescent intensity / area averaged across 5 replicates. Scale bars are 100 μm except where otherwise noted.

Figure S13. Temperature dependence on GP incorporation. Glycopolymers bearing cholesterol membrane anchors can be inserted into the membranes of living cells. A) To determine the temperature dependence of **GP** incorporation into the membranes of CHO Lec8 cells, cells were grown in 12-well plates and treated with **GP-PCL** or **GP-Ø** (2 μM, 1 hr) at increasing temperature (4 °C – 37 °C). Membrane incorporation was observed at all temperatures assayed and minimal internalization was observed at 4 °C. B) Micrographs captured at 40x on a Keyence BZX8000 epifluorescent microscope of **GP-PCL** membrane incorporation (2 μM, 1 hr) at each temperature.

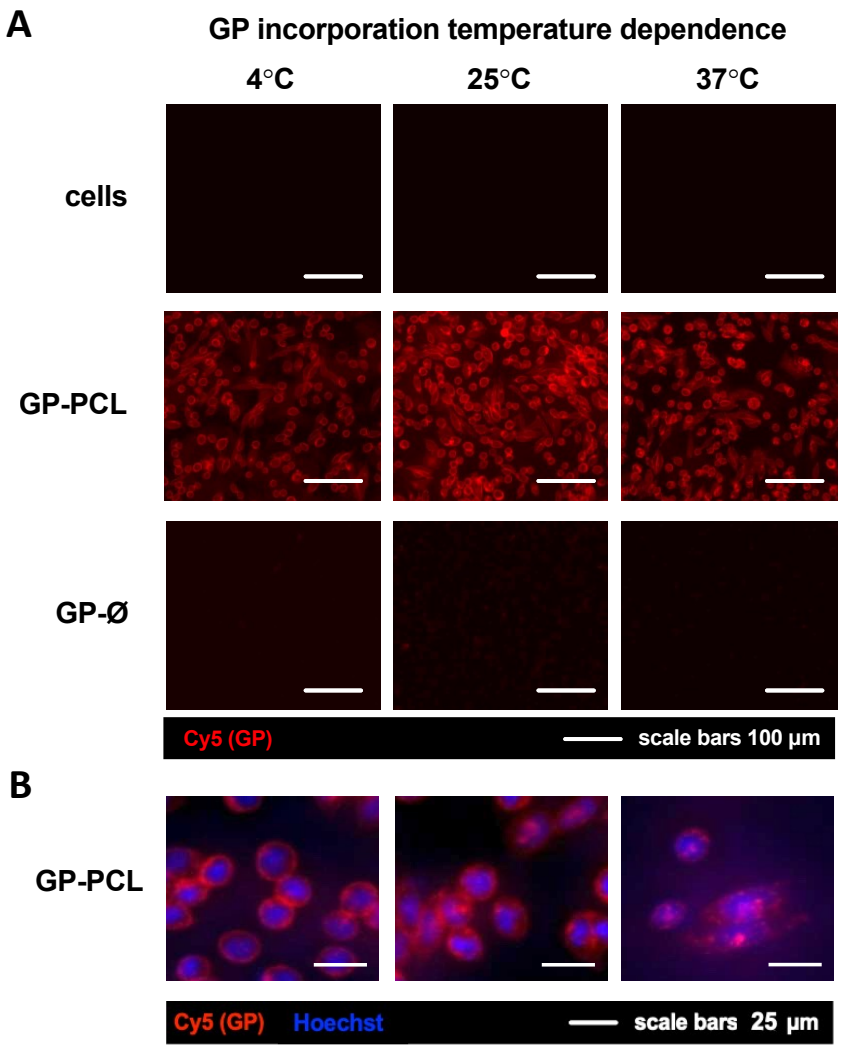

Figure S14. Cell viability during GP remodeling and photoshedding.

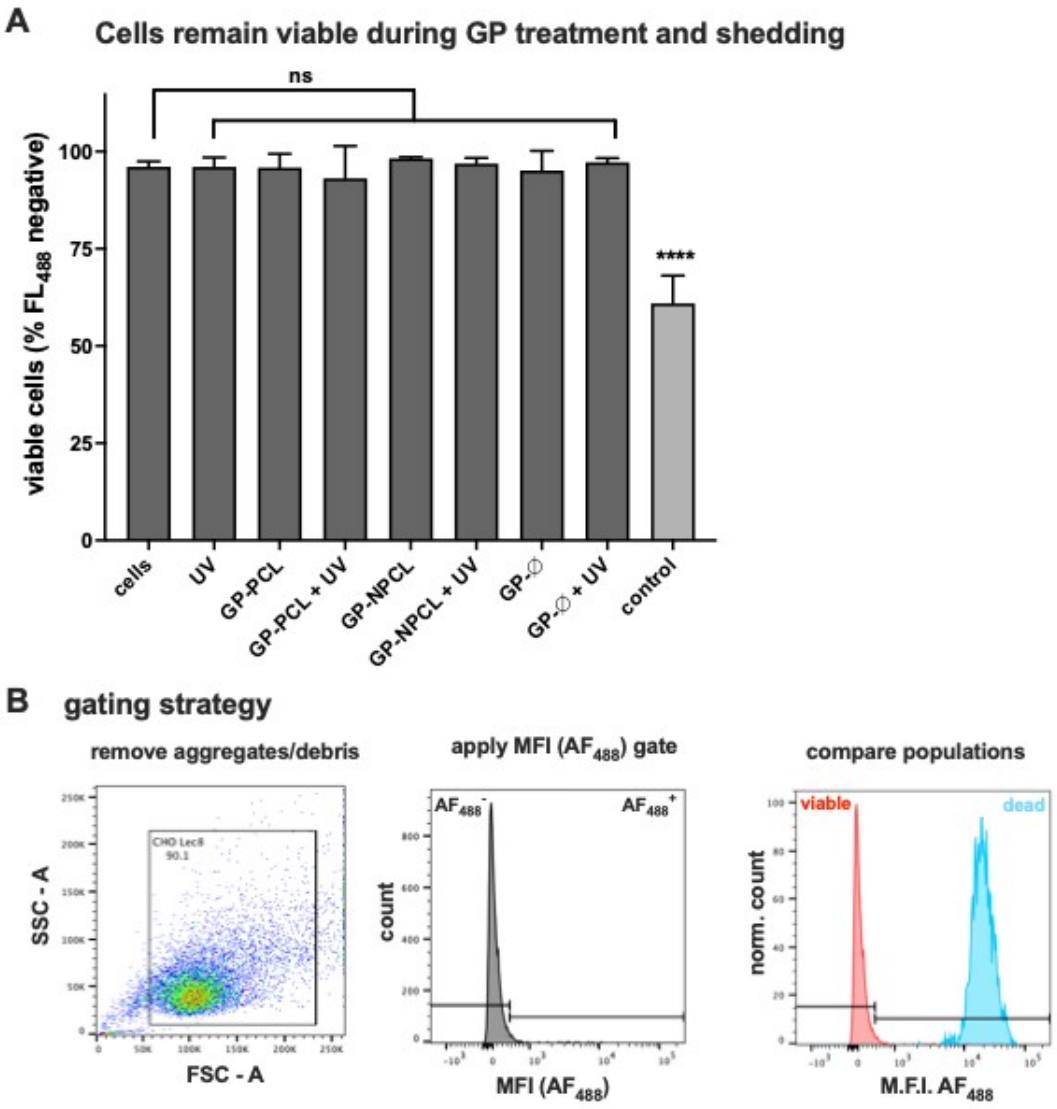

To assess cytotoxicity, a live-dead assay was performed using ThermoFisher Live/Dead fixable green dead cell stain kit (L34970). Briefly, 10^6 suspended CHO Lec8 cells were added to Eppendorf tubes. After remodeling cells using standard conditions described in this paper (2 μm, 0° C, 1 hr) with or without exposure to ultraviolet light (15W, λ = 365nm, 3 min), cells were pelleted and washed. To each pellet was added 1.00 uL of the dissolved, amine-reactive, dye in 1.00 mL of DPBS and cells were incubated for 30 min. Cells were washed twice with DPBS and resuspended for flow cytometry. Dead cells show increased MFI_{AF488} owing to increased

permeation of the dye across compromised cell membranes. The percentage of cells which remain viable (A) was identified following gating (B) of the cell population to remove debris and aggregates and then to identify dead cells. A control condition consisting of a 1:1 mixture of heat-treated cells (65° C, 2 min) and untreated cells was used to identify dead-cell population fluorescence levels. A sample histogram is shown overlayed with the MFI(AF_{488}) gate, showing a sample of untreated cells (red, viable) and a sample of heat-treated control cells (blue, dead).

Figure S15. RCA binding lactose competition assay. *wt* CHO cells (Pro5) were grown in 12-well plates. To demonstrate the binding specificity of RCA for lactose, cells were incubated with RCA (5 µg/mL, 0 °C, 40min) in the presence or absence of 200 mM soluble lactose. After three DPBS washes cells were and incubated with an excess of AlexaFluor488 labeled streptavidin (300µL, 1:750, 30 min) and then washed three additional times. Hoechst 33342 was used to visualize nuclei and the cells were imaged on a ThermoScientific EVOS imaging system. RCA binding was observed for Pro5 cells only in the absence of soluble lactose.

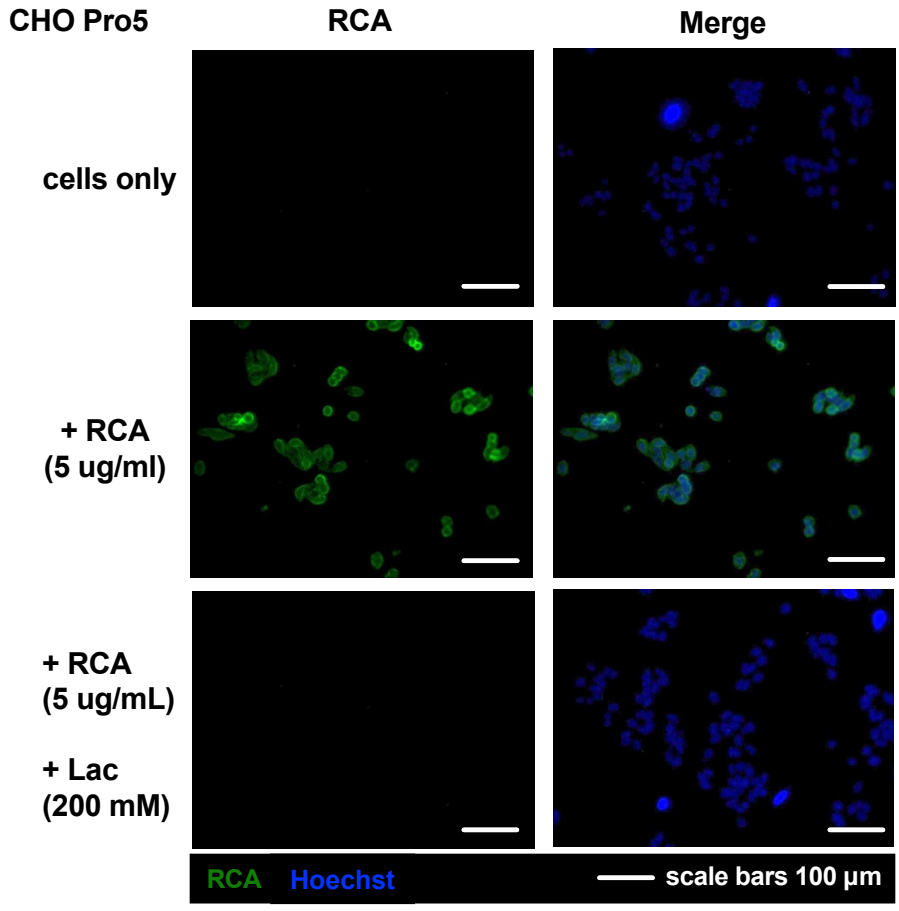

Figure S16. GP and RCA colocalize at the cell surface. To assess the colocalization of the lactosylated **GPs** with RCA at the cell surface, CHO Lec 8 cells in 12-well plates were remodeled with **GP-PCL** and **GP-NPCL** (2 μM, 0° C, 1 hr) and washed three times with DPBS. Cells were then incubated with RCA (5 μg/mL, 0° C, 40 min), washed three more times with DPBS, and incubated with an excess of AlexaFluor488 labeled streptavidin (300μL, 1:750, 30 min). The cells were washed, and fluorescent micrographs were captured using A) a ThermoScientific EVOS imaging system or B) a Leica SP8 confocal microscope with a 63x oil immersion lens (cells grown on glass insert). Strong colocalization between **GPs** and lectin signal was determined by Pearson's Correlation Coefficient (PCC) analyzed in Image J. C) CHO Lec8 cells before and after incubation with RCA to visualize GP-PCL membrane distribution.

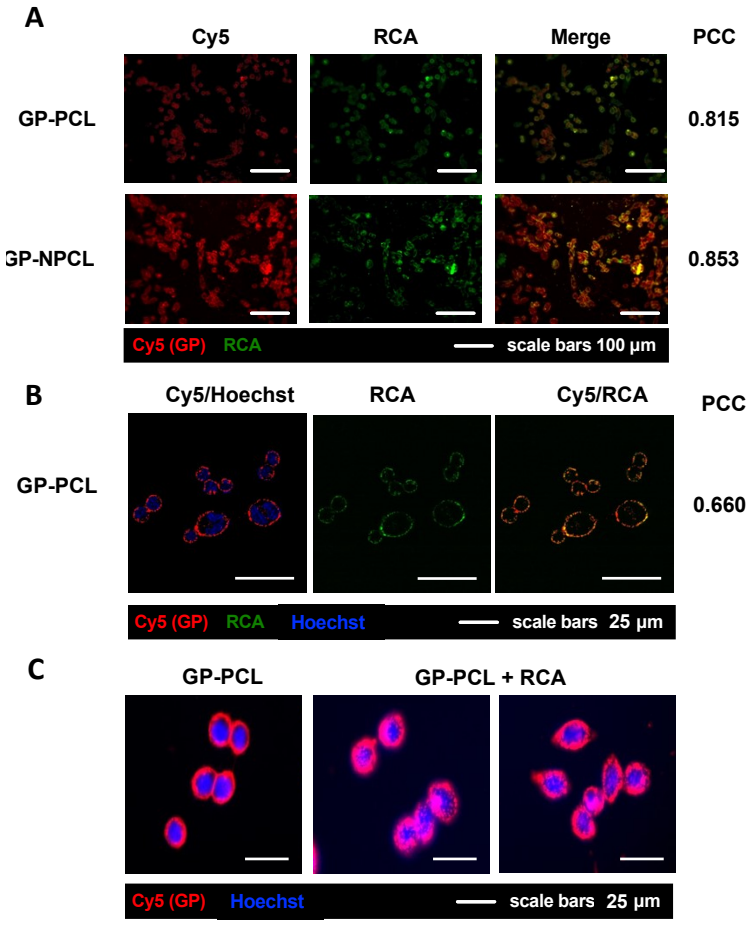

Figure S17. RCA binding optimization. To determine the optimal binding concentrations for RCA and lactose bearing glycoconjugates, flow cytometry (A) and fluorescent microscopy (B) were performed on *wt* CHO cells (Pro5). Dose-dependent RCA binding was observed by flow cytometry with a maximum signal without evidence of cell agglutination at 5 µg/mL RCA. This concentration was also suitable for fluorescent microscopy, where concentrations ranging from 0 - 50 µg/mL where evaluated and binding was visualized at concentrations above 2.5 µg/mL.

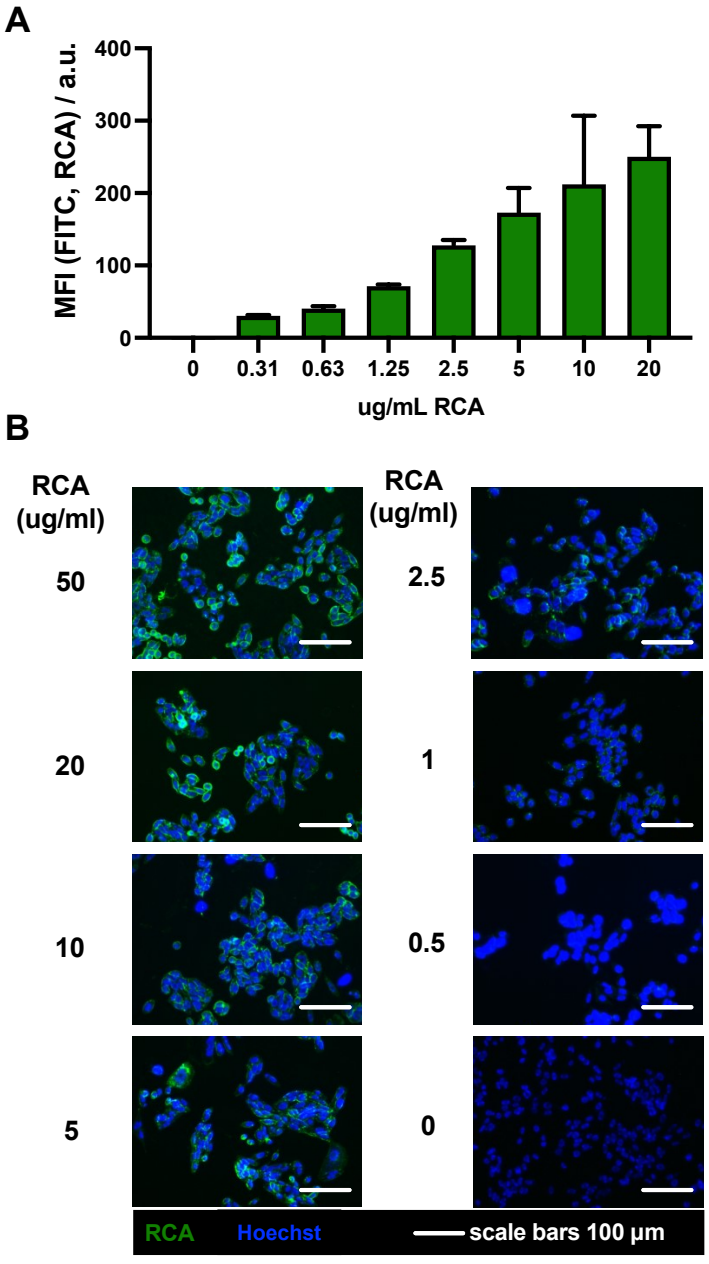

Figure S18. Expanded lectin crosslinking imaging panel. Additional images (included in the Fig4C quantitative analysis of lectin crosslinking) show that RCA crosslinking of the mucin mimetic **GP-PCL** stabilizes the synthetic glycocalyx to photoinduced shedding. Remodeled cells which were illuminated by ultraviolet light *prior* to RCA binding (UV pre) show reduced signal attributed to photolysis and clearance of **GPs** from the cell surface. Remodeled cells which were illuminated by ultraviolet light *following* RCA binding and crosslinking (UV post) show a retention of polymer and RCA signal, relative to a control not treated by UV light (no UV).

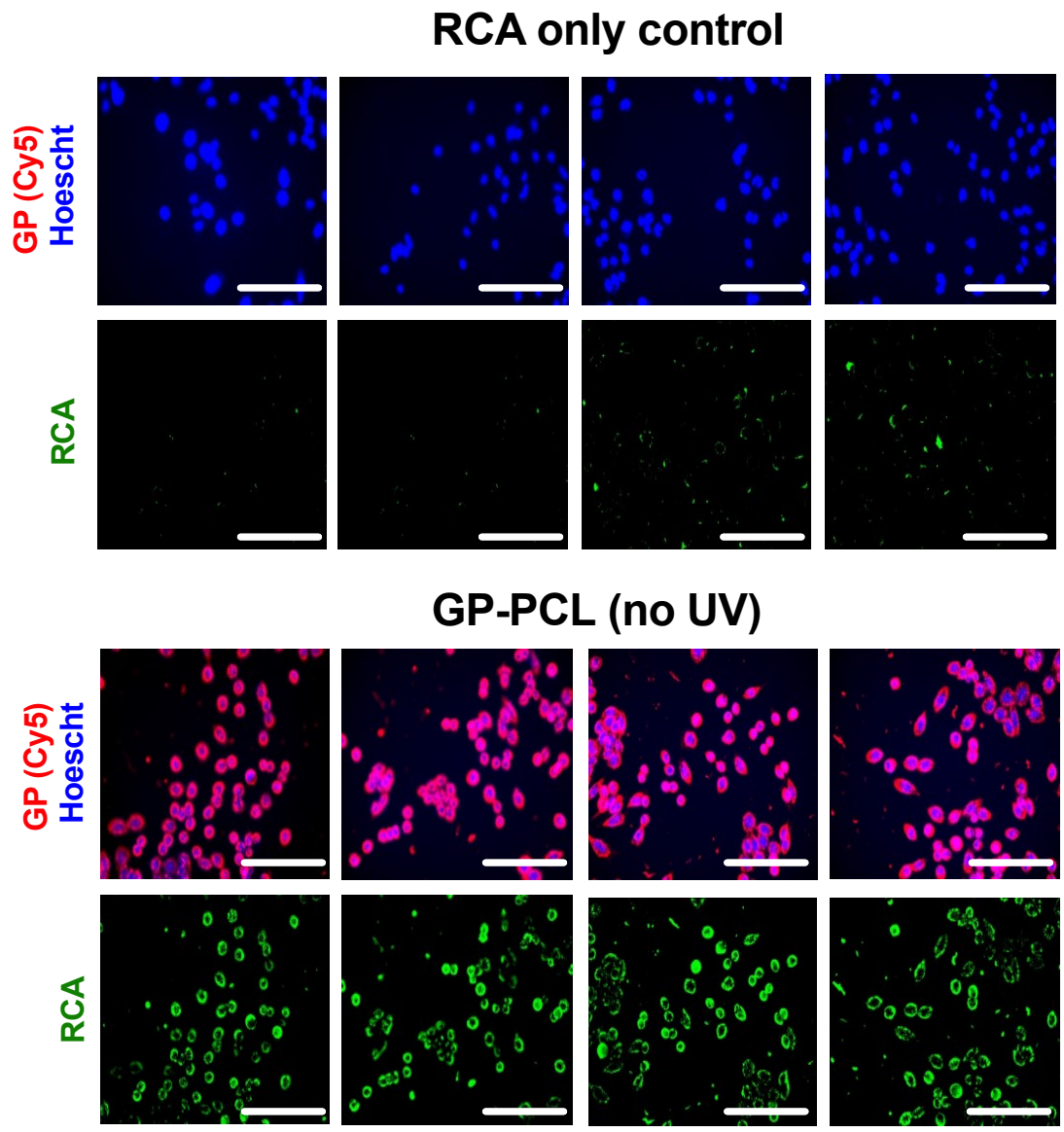

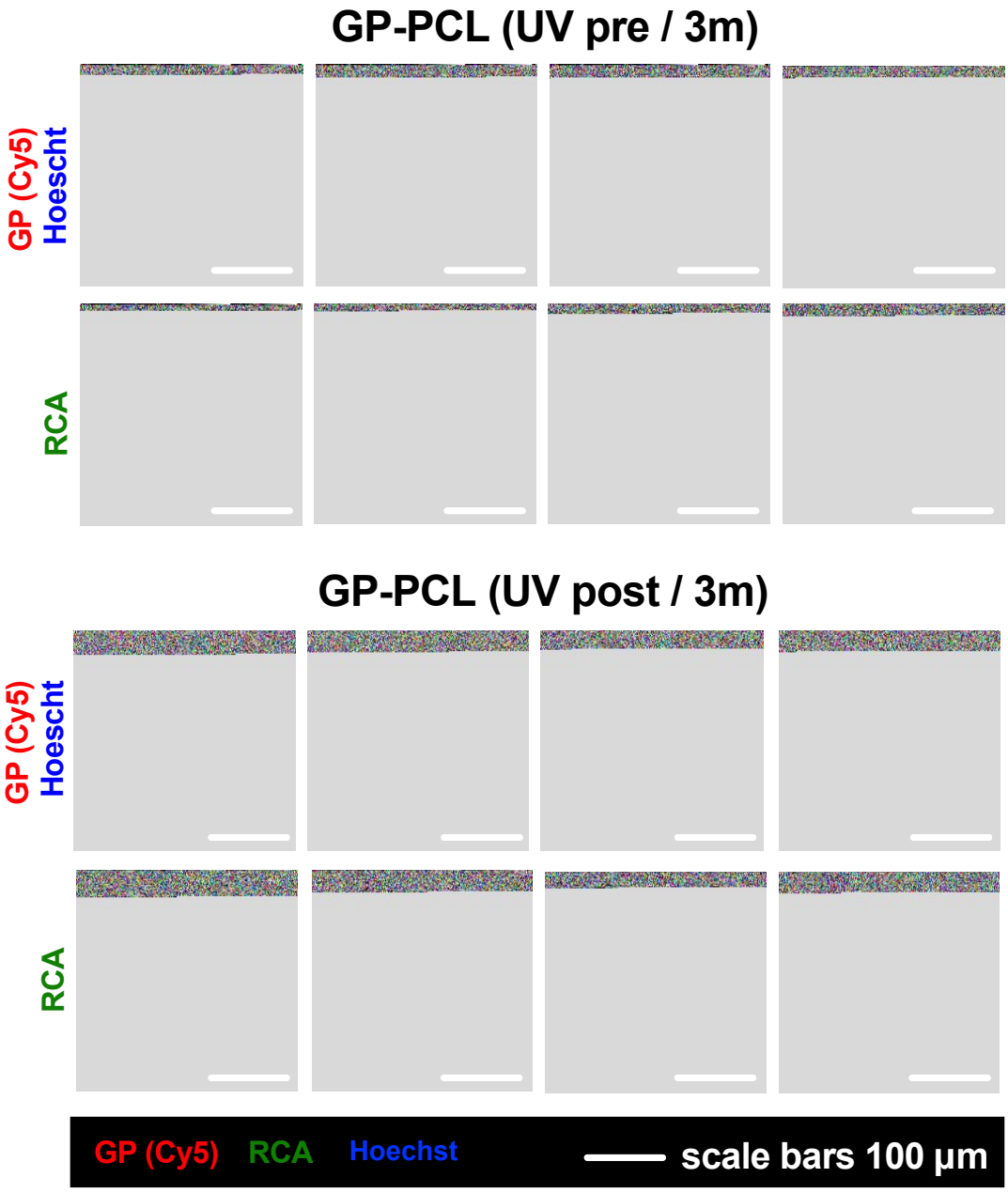
GP-PCL (UV pre / 3m)
GP (Cy5)
Hoescht
RCA
GP-PCL (UV post / 3m)
GP (Cy5)
Hoescht
RCA
GP (Cy5) RCA Hoechst
scale bars 100 µm

Figure S19. RCA binding to CHO cells by flow cytometry. CHO Pro5 or CHO Lec8 cells were suspended (0.25% trypsin-EDTA), washed, and 10^6 cells were pelleted in Eppendorf tubes. **GP-PCL** prepared in DPBS (0 or 1 uM, 100 µL) was added to the cell pellets after resuspension and incubated on ice for 1hr. Following two DPBS washes cells were incubated in RCA-biotin (5 ug/mL, 300µL) for 40 min on ice. After two additional washes cells were incubated in excess AlexaFluor488 labeled streptavidin (300µL, 1:750) for 20 min, washed twice with DPBS, and resuspended for flow cytometry analysis. A) CHO Pro5 cells bind RCA strongly in the absence of **GP-PCL**. B) CHO Lec8 cells show minimal RCA binding activity in the absence of **GP-PCL**, but binding is observed in the presence of **GP-PCL**.

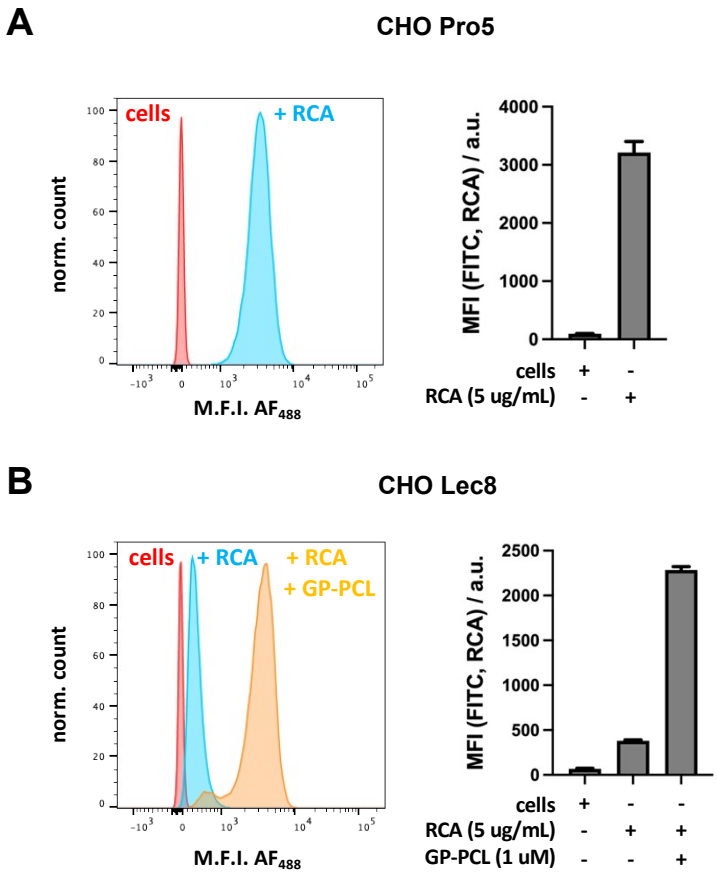

REFERENCES

1. D.J. Honigfort, M.O. Altman, P. Gagneux, K. Godula, *Proc. Nat'l. Acad. Sci.*, 2021, **118 (40)**, e2107896118, doi: 10.1073/pnas.2107896118.

2. M. Gervais, A. Labbé, S. Carlotti, A. Deffieux, *Macromolecules.* 2009, **42(7)**, 2395–2400, doi: 10.1021/ma802063s.

3. S. Kaneko, H. Nakayama, Y. Yoshino, D. Fushimi, K. Yamaguchi, Y. Horiike, J. Nakanishi, *Phys Chem Chem Phys.* 2011, **13(9)**, 4051- 4059, doi: 10.1039/C0CP02013C.

4. S. Isabettini, M. Liebi, J. Kohlbrecher, T. Ishikawa, P. Fischer, E.J. Windhab, P. Walde, S. Kuster, *Phys Chem Chem Phys.* 2017, **19(17)**, 10820- 10824, doi: 10.1039/C7CP01025G.

5. J. Eirich, R. Orth, S.A. Sieber, *J. Am. Chem. Soc.*, 2011, **133(31)**, 12144-12153, doi: 10.1021/ja2039979.